CLEO CONF 97-31
EPS97 368

# The Hadronic Current in Tau Lepton Decay to Two Pseudoscalar Mesons

CLEO Collaboration

(August 14, 1997)

## Abstract

We report on studies of the invariant mass spectra of the hadronic systems in the decays $\tau^- \to \pi^-\pi^0\nu_\tau$ and $\tau^- \to K_S^0\pi^-\nu_\tau$. These studies were performed using data obtained with the CLEO-II detector operating at the CESR $e^+e^-$ collider. In addition to results from fits to phenomenological models, we present comparisons with data on $e^+e^- \to \pi^+\pi^-$ as a test of CVC.

J. Bartelt,[1] S. E. Csorna,[1] V. Jain,[1,*] K. W. McLean,[1] S. Marka,[1] R. Godang,[2]
K. Kinoshita,[2] I. C. Lai,[2] P. Pomianowski,[2] S. Schrenk,[2] G. Bonvicini,[3] D. Cinabro,[3]
R. Greene,[3] L. P. Perera,[3] G. J. Zhou,[3] B. Barish,[4] M. Chadha,[4] S. Chan,[4] G. Eigen,[4]
J. S. Miller,[4] C. O'Grady,[4] M. Schmidtler,[4] J. Urheim,[4] A. J. Weinstein,[4] F. Würthwein,[4]
D. W. Bliss,[5] G. Masek,[5] H. P. Paar,[5] S. Prell,[5] V. Sharma,[5] D. M. Asner,[6] J. Gronberg,[6]
T. S. Hill,[6] D. J. Lange,[6] S. Menary,[6] R. J. Morrison,[6] H. N. Nelson,[6] T. K. Nelson,[6]
C. Qiao,[6] J. D. Richman,[6] D. Roberts,[6] A. Ryd,[6] M. S. Witherell,[6] R. Balest,[7]
B. H. Behrens,[7] W. T. Ford,[7] H. Park,[7] J. Roy,[7] J. G. Smith,[7] J. P. Alexander,[8] C. Bebek,[8]
B. E. Berger,[8] K. Berkelman,[8] K. Bloom,[8] D. G. Cassel,[8] H. A. Cho,[8] D. S. Crowcroft,[8]
M. Dickson,[8] P. S. Drell,[8] K. M. Ecklund,[8] R. Ehrlich,[8] A. D. Foland,[8] P. Gaidarev,[8]
R. S. Galik,[8] L. Gibbons,[8] B. Gittelman,[8] S. W. Gray,[8] D. L. Hartill,[8] B. K. Heltsley,[8]
P. I. Hopman,[8] J. Kandaswamy,[8] P. C. Kim,[8] D. L. Kreinick,[8] T. Lee,[8] Y. Liu,[8]
G. S. Ludwig,[8] N. B. Mistry,[8] C. R. Ng,[8] E. Nordberg,[8] M. Ogg,[8,†] J. R. Patterson,[8]
D. Peterson,[8] D. Riley,[8] A. Soffer,[8] B. Valant-Spaight,[8] C. Ward,[8] M. Athanas,[9] P. Avery,[9]
C. D. Jones,[9] M. Lohner,[9] C. Prescott,[9] J. Yelton,[9] J. Zheng,[9] G. Brandenburg,[10]
R. A. Briere,[10] A. Ershov,[10] Y. S. Gao,[10] D. Y.-J. Kim,[10] R. Wilson,[10] H. Yamamoto,[10]
T. E. Browder,[11] Y. Li,[11] J. L. Rodriguez,[11] T. Bergfeld,[12] B. I. Eisenstein,[12] J. Ernst,[12]
G. E. Gladding,[12] G. D. Gollin,[12] R. M. Hans,[12] E. Johnson,[12] I. Karliner,[12] M. A. Marsh,[12]
M. Palmer,[12] M. Selen,[12] J. J. Thaler,[12] K. W. Edwards,[13] A. Bellerive,[14] R. Janicek,[14]
D. B. MacFarlane,[14] P. M. Patel,[14] A. J. Sadoff,[15] R. Ammar,[16] P. Baringer,[16] A. Bean,[16]
D. Besson,[16] D. Coppage,[16] C. Darling,[16] R. Davis,[16] N. Hancock,[16] S. Kotov,[16]
I. Kravchenko,[16] N. Kwak,[16] S. Anderson,[17] Y. Kubota,[17] S. J. Lee,[17] J. J. O'Neill,[17]
S. Patton,[17] R. Poling,[17] T. Riehle,[17] V. Savinov,[17] A. Smith,[17] M. S. Alam,[18]
S. B. Athar,[18] Z. Ling,[18] A. H. Mahmood,[18] H. Severini,[18] S. Timm,[18] F. Wappler,[18]
A. Anastassov,[19] J. E. Duboscq,[19] D. Fujino,[19,‡] K. K. Gan,[19] T. Hart,[19] K. Honscheid,[19]
H. Kagan,[19] R. Kass,[19] J. Lee,[19] M. B. Spencer,[19] M. Sung,[19] A. Undrus,[19,§] R. Wanke,[19]
A. Wolf,[19] M. M. Zoeller,[19] B. Nemati,[20] S. J. Richichi,[20] W. R. Ross,[20] P. Skubic,[20]
M. Bishai,[21] J. Fast,[21] J. W. Hinson,[21] N. Menon,[21] D. H. Miller,[21] E. I. Shibata,[21]
I. P. J. Shipsey,[21] M. Yurko,[21] S. Glenn,[22] S. D. Johnson,[22] Y. Kwon,[22,**] S. Roberts,[22]
E. H. Thorndike,[22] C. P. Jessop,[23] K. Lingel,[23] H. Marsiske,[23] M. L. Perl,[23] D. Ugolini,[23]
R. Wang,[23] X. Zhou,[23] T. E. Coan,[24] V. Fadeyev,[24] I. Korolkov,[24] Y. Maravin,[24]
I. Narsky,[24] V. Shelkov,[24] J. Staeck,[24] R. Stroynowski,[24] I. Volobouev,[24] J. Ye,[24]
M. Artuso,[25] A. Efimov,[25] M. Goldberg,[25] D. He,[25] S. Kopp,[25] G. C. Moneti,[25]
R. Mountain,[25] S. Schuh,[25] T. Skwarnicki,[25] S. Stone,[25] G. Viehhauser,[25] and X. Xing[25]

[*]Permanent address: Brookhaven National Laboratory, Upton, NY 11973.

[†]Permanent address: University of Texas, Austin TX 78712

[‡]Permanent address: Lawrence Livermore National Laboratory, Livermore, CA 94551.

[§]Permanent address: BINP, RU-630090 Novosibirsk, Russia.

[**]Permanent address: Yonsei University, Seoul 120-749, Korea.

[1]Vanderbilt University, Nashville, Tennessee 37235
[2]Virginia Polytechnic Institute and State University, Blacksburg, Virginia 24061
[3]Wayne State University, Detroit, Michigan 48202
[4]California Institute of Technology, Pasadena, California 91125
[5]University of California, San Diego, La Jolla, California 92093
[6]University of California, Santa Barbara, California 93106
[7]University of Colorado, Boulder, Colorado 80309-0390
[8]Cornell University, Ithaca, New York 14853
[9]University of Florida, Gainesville, Florida 32611
[10]Harvard University, Cambridge, Massachusetts 02138
[11]University of Hawaii at Manoa, Honolulu, Hawaii 96822
[12]University of Illinois, Champaign-Urbana, Illinois 61801
[13]Carleton University, Ottawa, Ontario, Canada K1S 5B6
and the Institute of Particle Physics, Canada
[14]McGill University, Montréal, Québec, Canada H3A 2T8
and the Institute of Particle Physics, Canada
[15]Ithaca College, Ithaca, New York 14850
[16]University of Kansas, Lawrence, Kansas 66045
[17]University of Minnesota, Minneapolis, Minnesota 55455
[18]State University of New York at Albany, Albany, New York 12222
[19]Ohio State University, Columbus, Ohio 43210
[20]University of Oklahoma, Norman, Oklahoma 73019
[21]Purdue University, West Lafayette, Indiana 47907
[22]University of Rochester, Rochester, New York 14627
[23]Stanford Linear Accelerator Center, Stanford University, Stanford, California 94309
[24]Southern Methodist University, Dallas, Texas 75275
[25]Syracuse University, Syracuse, New York 13244

## I. INTRODUCTION

The $\tau$ is the only lepton heavy enough to decay to final states containing hadrons. Since leptons do not participate in the strong interaction, $\tau$ lepton decay is uniquely suited for studying low energy hadronic dynamics. Furthermore, angular momentum conservation plus the transformation properties under parity and G-parity of the vector and axial vector parts of the weak current give rise to selection rules that constrain the types of hadronic states that may form. Thus, $\tau$ lepton decay provides an especially clean environment for studying these states. In this contribution, we present preliminary studies made using the CLEO-II detector of the $\pi\pi$ and $\overline{K}\pi$ systems [1] in the decays $\tau^- \to \pi^-\pi^0\nu_\tau$ and $\tau^- \to K_S^0\pi^-\nu_\tau$.

In semi-hadronic $\tau$ decay, final states consisting of two pseudoscalars may only have $J^P = 0^+$ or $1^-$. Furthermore, the Conserved Vector Current theorem (CVC) forbids production of $0^+$ non-strange states in $\tau$ decay. Thus, the rate for the decay $\tau^- \to \pi^-\pi^0\nu_\tau$ can be written as a function of the $\pi^-\pi^0$ effective mass squared $q^2$ as [2]:

$$\frac{d\Gamma(\tau \to \nu\pi\pi^0)}{dq^2} = \frac{G_F^2\,|V_{ud}|^2}{32\pi^2\,M_\tau^3}(M_\tau^2 - q^2)^2\,(M_\tau^2 + 2q^2)\,v_1^{\pi\pi}(q^2), \tag{1}$$

where $v_1^{\pi\pi}(q^2)$, representing that part of the vector spectral function responsible for production of the $\pi\pi^0$ system, contains the hadronic dynamics. CVC relates $v_1^{\pi\pi}(q^2)$ to the isovector contribution to the $e^+e^- \to \pi^+\pi^-$ cross-section, up to isospin-violating effects:

$$\sigma^{(I=1)}_{ee\to\pi^+\pi^-}(q^2) = \frac{4\pi^2\alpha^2}{q^2}\,v_1^{\pi\pi}(q^2). \tag{2}$$

This cross-section is directly related to the pion electromagnetic form factor $F_\pi(q^2)$:

$$\sigma_{ee\to\pi^+\pi^-}(q^2) = \frac{\pi\alpha^2}{3q^2}\,\left|F_\pi(q^2)\right|^2\,\left(\frac{2p_\pi}{\sqrt{q^2}}\right)^3, \tag{3}$$

where the last factor represents the P-wave phase space factor, with $p_\pi$ being the momentum of one of the pions in the $\pi\pi$ rest frame.

In addition to comparing directly with the low-energy $e^+e^-$ data as a test of CVC, one can analyze the $\pi\pi^0$ mass spectrum from $\tau$ decay in the context of phenomenological models for $F_\pi$, or equivalently $v_1^{\pi\pi}$. The pion form factor is defined such that $F_\pi(q^2 = 0) = 1$, but is otherwise not rigorously specified by theory. In the picture of resonance dominance, the $\pi\pi^0$ mass spectrum will have its largest contribution from the lowest lying isospin-1 vector meson, the $\rho(770)$, with additional contributions possible from radial excitations such as the $\rho'(1450)$ and $\rho''(1700)$. In the simple model of Kühn and Santamaria (K&S) [3], this is written as

$$F^{(I=1)}_{\pi\pi}(q^2) = \frac{1}{1+\beta+\gamma+\cdots}\,(BW_\rho + \beta\,BW_{\rho'} + \gamma\,BW_{\rho''} + \cdots), \tag{4}$$

where $BW_\rho = M_\rho^2/[(M_\rho^2 - q^2) - i\sqrt{q^2}\Gamma_\rho(q^2)]$ represents the Breit-Wigner associated with the $\rho(770)$ propagator, and $\beta$ and $\gamma$ specify the relative couplings for $\rho'$ and $\rho''$. Considering the case where $\beta$ and $\gamma$ are both zero, the spectral function can be expressed (following Tsai) [2] as:

$$v_1^{\pi\pi}(q^2) = \frac{2\pi f_\rho^2}{q^2}\left[\frac{\sqrt{q^2}\,\Gamma_\rho(q^2)/\pi}{(M_\rho^2 - q^2)^2 + q^2\,\Gamma_\rho(q^2)^2}\right], \tag{5}$$

where $\Gamma_\rho(q^2) = (g_\rho^2/48\pi)\sqrt{q^2}\,(2p_\pi/\sqrt{q^2}\,)^3$ gives the energy dependence of the $\rho$ width. The constants $f_\rho$ (with units of mass$^2$) and $g_\rho$ (dimensionless) can be identified as the weak and strong $\rho$ meson decay constants, respectively. In the chiral limit, $f_\rho g_\rho = \sqrt{2}M_\rho^2$.

Analogous considerations hold for the decay $\tau^- \to K_S\pi^-\nu_\tau$ [4–6]. The dominant contribution is expected to be from the $K^*(892)$ meson, but radial excitations like the $K^{*\prime}(1410)$ may be present as well. CVC cannot be applied directly to states with net strangeness; instead one must rely on SU(3) flavor symmetry to relate $\overline{K}\pi$ and $\pi\pi$ production. The approximate nature of SU(3) alters the situation somewhat: for example, unlike in the $\pi^-\pi^0$ case, scalar resonances such as the $K_0^*(1430)$ are permitted to contribute.

Here we analyze the $\pi^-\pi^0$ and $K_S\pi^-$ mass spectra in the context of the K&S model described above to address some of these issues. Specifically, we determine the resonance parameters and relative couplings that appear in Eqs. 4 and 5. We do not directly consider the possibility of non-resonant contributions to these final states. In the $\pi^-\pi^0$ case, we compare the mass spectrum from $\tau$ decay with the cross-section for $e^+e^- \to \pi^+\pi^-$ obtained by other experiments, as a test of CVC. Finally, we note that studies of angular distributions permit the separation of possible scalar contributions. Such studies are in progress and will not be reported here.

In the following section, we describe the event selection procedure for the two decay modes under study. For the purposes of comparing with $e^+e^-$ data and fitting to various phenomenological models, we are motivated to present the invariant mass spectra from the data as histograms which have been corrected for backgrounds and distortions due primarily to detector effects. We describe the procedures used to correct the data in Section III. Studies of the corrected $\tau^- \to \pi^-\pi^0\nu_\tau$ data are presented in Section IV, and those for the $K_S\pi$ mode are presented in Section V.

## II. EVENT SELECTION

The data described here were collected with the CLEO-II detector operating at the CESR $e^+e^-$ storage ring at center-of-mass energy $\sqrt{s} \sim 10.6$ GeV. CLEO-II [8] consists of three concentric cylindrical drift chambers surrounded by scintillation counters used primarily for triggering and an array of 7800 CsI(Tl) crystals for electromagnetic calorimetry. These components are enclosed within a superconducting solenoid with an axial magnetic field of 1.5 Tesla. Plastic streamer tubes are deployed at three depths in the surrounding magnet iron for muon identification.

### A. Selection of $\pi^-\pi^0$ Events

We select $\tau^- \to h^-\pi^0\nu_\tau$ candidates [7] in $\tau$-pair events tagged by the recoiling $\tau^+$ decay to $e^+\nu_e\overline{\nu}_\tau$, $\mu^+\nu_\mu\overline{\nu}_\tau$, or $h^+\pi^0\overline{\nu}_\tau$, as described in Ref. [9]. For this analysis we use 3.31 fb$^{-1}$ of CLEO-II data, corresponding to $3.02 \times 10^6$ produced $\tau$-pair events. Figure 1 shows the normalized $M_{\gamma\gamma}$ distribution for pairs of photons forming the $\pi^0$ candidates in lepton-tagged events. We require $M_{\gamma\gamma}$ to be within $2\sigma$ of the $\pi^0$ mass, where $\sigma$ is typically 4–7 MeV. We apply the $\pi^0$ mass constraint to improve the $\pi^0$ energy resolution. No attempt is made to distinguish the small admixture of $\tau^- \to K^-\pi^0\nu_\tau$ decays entering the sample, given limited $\pi/K$ separation capabilities at CLEO.

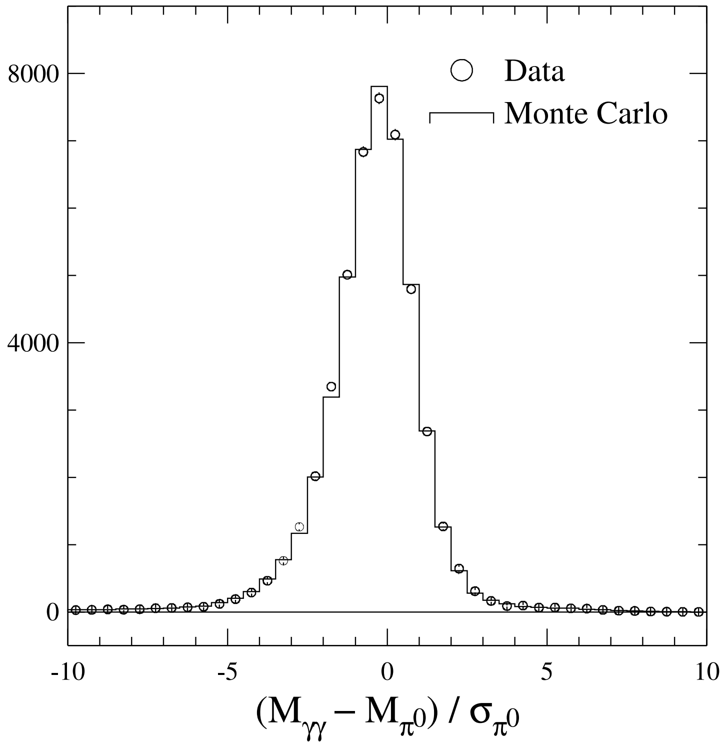


FIG. 1. Normalized $M_{\gamma\gamma}$ distribution for photon pairs in lepton-tagged $\tau^- \to h^-\pi^0\nu_\tau$ candidate events (points). The histogram overlaid represents the $\tau\tau$ MC expectation.

With this selection, roughly 69,000 $\tau^- \to \pi^-\pi^0\nu_\tau$ candidates remain. Of these, $\sim$ 2% are $\tau$ decays with spuriously reconstructed $\pi^0$'s, as estimated from the side bands in Fig. 1. An additional 4.5% are estimated from the Monte Carlo (MC) to be feeddown from other $\tau$ decays with a real $\pi^0$, primarily decays to $\pi^-\pi^0\pi^0\nu_\tau$, $K^-\pi^0\nu_\tau$ and $K_L^0 h^-\pi^0\nu_\tau$.

### B. Selection of $K_S\pi^-$ Events

We select $\tau^- \to K_S^0\pi^-\nu_\tau$ decays recoiling against $e^+\nu_e\overline{\nu}_\tau$, $\mu^+\nu_\mu\overline{\nu}_\tau$, $h^+\overline{\nu}_\tau$, and $h^+\pi^0\overline{\nu}_\tau$ tags, following criteria described in Ref. [10]. For this analysis, we use a larger sample of CLEO-II data, corresponding to $4.4 \times 10^6$ produced $\tau$-pair events.

In contrast with the $\pi^-\pi^0$ case where statistics are high even after stringent selection criteria, we relax geometric and kinematic cuts to achieve high acceptance. However, the $K_S\pi^-$ channel has a more serious problem with backgrounds, and thus we apply several additional cuts targeting specific sources. First to reduce contamination from events without a real $K_S$, we require both pions forming the $K_S$ to be inconsistent with originating from the

$e^+e^-$ interaction point (IP). That is, we require their impact parameters relative to the IP in the plane transverse to the beam axis to exceed 0.5 mm. Also, we reduce background from $\tau^- \to K^- K_S \nu_\tau$, by making a tight cut on the $dE/dx$ measurement of the track accompanying the $K_S$.

The $M_{\pi^+\pi^-}$ distribution for $K_S$ candidates is shown in Figure 2, with the cut on this quantity relaxed. After all cuts, 1265 candidate events remain. Of these, the residual background is $\sim 25\%$, primarily from $\tau$ decays to $K^- K_S \nu_\tau$, $K_S K_L \pi^- \nu_\tau$, and $K_S \pi^- \pi^0 \nu_\tau$. For determination of the $M_{K_S \pi^-}$ mass spectrum, we recompute the track parameters of the pions forming the $K_S$ candidate, employing $K_S$ mass and vertex constraints.

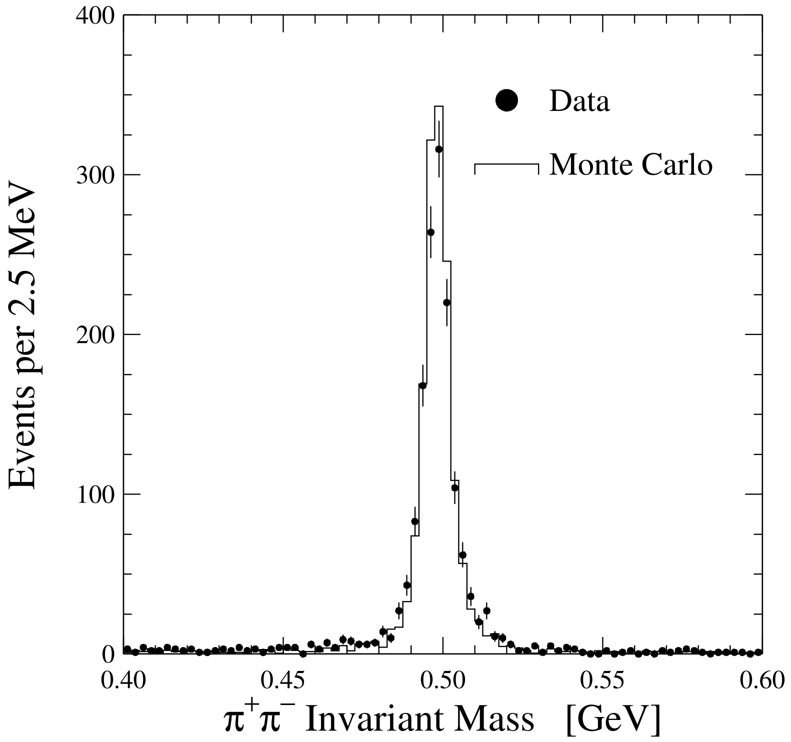


FIG. 2. $M_{\pi^+\pi^-}$ distribution for $K_S^0$ candidates (points). Overlaid is the corresponding $\tau\tau$ MC spectrum.

## III. CORRECTIONS

Before studying the $\pi^-\pi^0$ and $K_S\pi^-$ mass spectra, the raw spectra must be corrected for three experimental effects that may cause distortions: (1) backgrounds, (2) smearing due to resolution and radiative effects, and (3) mass-dependence of the experimental acceptance. In this section, we describe these corrections as applied to the $M_{\pi^-\pi^0}$ spectrum. These corrections rely primarily on the Monte Carlo simulation of the physics and detector response. The physics of the tau-pair production and decay is modelled using the `KORALB/TAUOLA` event generator [11], and the detector response is handled using a `GEANT`-based [12] simulation of the CLEO-II detector.

### A. Corrections for Backgrounds

As noted earlier, the backgrounds entering the $\tau^- \to \pi^-\pi^0\nu_\tau$ sample are small. Sidebands in the $M_{\gamma\gamma}$ distribution are used to model the fake-$\pi^0$ contribution. The remaining 4.5% are modeled using the $\tau$-pair Monte Carlo sample.

### B. Correction for Bin Migration

Detector resolution causes the $\pi^-\pi^0$ mass spectrum to become broader. The presence of radiation in the decay $\tau^- \to \pi^-\pi^0[\gamma]\nu_\tau$ broadens and shifts the spectrum. We correct for these effects by performing an approximate unfold, based on a bin migration matrix determined from the $\tau^- \to \pi^-\pi^0\nu_\tau$ MC sample. Since the experimental resolution on $M_{\pi\pi^0}$ is dominated by that on the $\pi^0$ energy, the good agreement between data and MC shown in Fig. 1 gives us confidence in this aspect of the correction procedure. For the radiative effect, we rely on the `PHOTOS`-based simulation [13] employed by `TAUOLA`.

### C. Correction for Acceptance

Finally we correct for mass dependence of the acceptance. Again, this is determined from the MC simulation. The main effects causing this dependence are associated with the kinematics of the decay and the cuts imposed in the event selection, both of which are well understood.

## IV. THE $\pi^-\pi^0$ MASS SPECTRUM

### A. Fits to the K&S Model

We perform simple $\chi^2$ fits to the fully-corrected $\pi^-\pi^0$ mass spectrum to extract resonance parameters and couplings, as illustrated in Figure 3. Because of poor statistics and/or large uncertainties in the background estimation, only data in the range 0.5 to 1.5 GeV are included in the fits. Also, as a result of the unfolding procedure, off-diagonal terms of the covariance matrix are non-zero, and the corresponding terms are included in the calculation of the $\chi^2$ being minimized. However, the off-diagonal terms are not reflected in the error bars shown in Fig. 3.

We fit using the functional form for $v_1^{\pi\pi}$ described in the introduction (the K&S model), but only allowing for $\rho$ and $\rho'$ contributions. Since this is the model used in the `KORALB/TAUOLA` event generator [11], comparisons between data and Monte Carlo are facillitated. The effects of including a $\rho''$ contribution and modifying the energy dependence of the meson widths are considered in Section IV C. Thus, the free parameters in the fit are the normalization, the masses ($M_\rho$ and $M_{\rho'}$), the pole widths ($\Gamma_\rho \equiv \Gamma_\rho(q^2 = M_\rho^2)$ and similarly $\Gamma_{\rho'}$), and the $\rho'$ admixture parameter $\beta$. The decay constants $f_\rho$ and $g_\rho$ (and those for the $\rho'$) are thus absorbed into the definitions of normalization, pole widths and $\beta$.

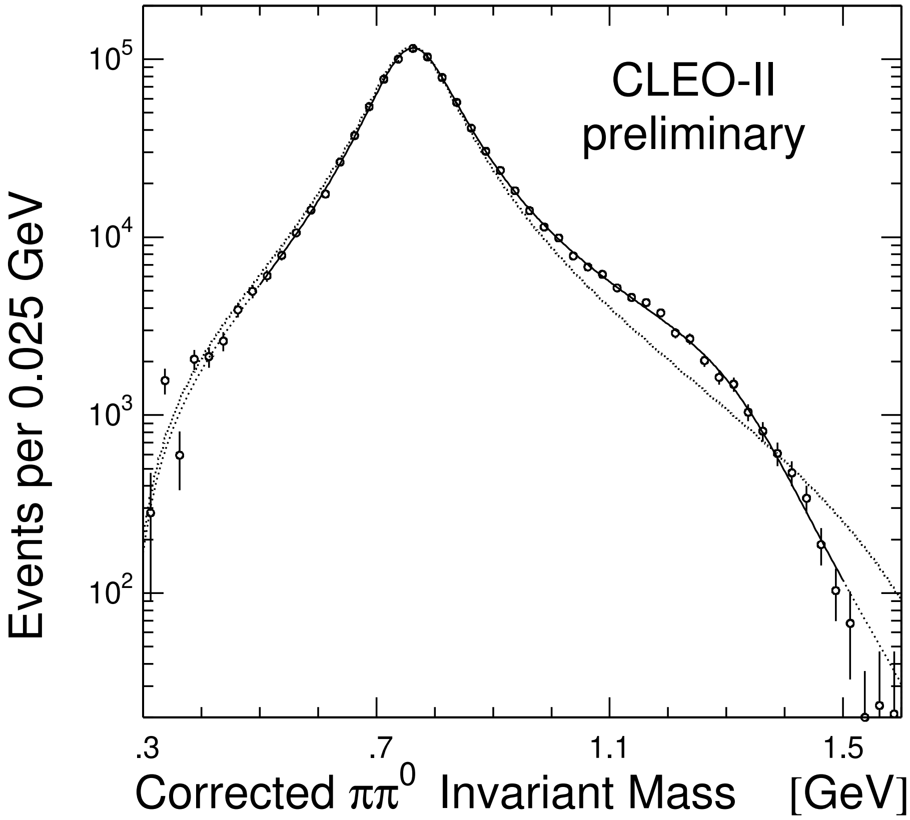


FIG. 3. Fully corrected $M_{\pi^-\pi^0}$ distribution in $\tau^- \to \pi^-\pi^0\nu_\tau$ events (points). The solid curve overlaid represents the results of the fit to the K&S model. The dotted curve is obtained using the $\rho(770)$ parameters obtained from the fit, but with the $\rho'$ contribution turned off (*i.e.*, $\beta$ set to zero).

Although interfering amplitudes may in general differ by a phase, $\beta$ is expected to be real so that the pion form factor will be real at $q^2 = 0$. We have checked this by including an imaginary component of $\beta$ as a separate parameter in the fit. We find this parameter to be consistent with zero. Thus, in all fits described here we have fixed the imaginary part of $\beta$ to be zero.

Preliminary results for the $\pi^-\pi^0$ lineshape parameters are given in in Table I. The estimation of systematic errors is discussed in the following section. For comparison, we also show in Table I the results from the K&S fits to the $e^+e^-$ data in which a non-zero $\rho''$ contribution is permitted. The $\rho''$ component is essential here since the $e^+e^-$ data extend to higher values of $s = q^2$ than the $\tau$ data. The errors on the fit parameters are not directly quoted in Ref. [3], however from comments therein and from fits by other authors to similar functional forms [14,15], we conclude that the precision of the CLEO $\tau$ data is comparable to that of the $e^+e^-$ data.

The fit function we use differs from that employed by Kühn and Santamaria [3] to fit the $e^+e^- \to \pi^+\pi^-$ data, however, in that we impose no constraint on the normalization to ensure that $F_\pi(q^2 = 0) = 1$. Imposing such a constraint will affect the fit parameters somewhat, and so the comparison in Table I is not ideal. Using the world average value for

TABLE I. Results from fits to $e^+e^- \to \pi^+\pi^-$ and $\tau^- \to \pi^-\pi^0\nu_\tau$ data. All values are in units of MeV, except for $\beta$. For the CLEO results, the first error listed is the statistical error, while the second is the systematic error; for the ALEPH results the error listed is due to statistics and systematics combined.

| | K&S ($e^+e^-$) | CLEO-II ($\tau$) | ALEPH ($\tau$) |
|---|---|---|---|
| $M_\rho$ | 773 | $774.3 \pm 0.7 \pm 0.9$ | $774.9 \pm 0.9$ |
| $\Gamma_\rho$ | 144 | $149.1 \pm 1.4 \pm 0.8$ | $144.2 \pm 1.5$ |
| $M_{\rho'}$ | 1320 | $1370 \pm 10 \pm 6$ | $1363 \pm 15$ |
| $\Gamma_{\rho'}$ | 390 | $386 \pm 39 \pm 18$ | $\equiv 310$ |
| $\beta$ | $-0.103$ | $-0.091 \pm 0.008 \pm 0.004$ | $-0.094 \pm 0.007$ |
| $\chi^2$/dof | 136/132 | 22.4/34 | 81/65 |

the $\tau^- \to \pi^-\pi^0\nu_\tau$ branching fraction [16] and the normalization obtained from the fit, our fit function extrapolates to $|F_\pi(q^2 = 0)|^2 = 1.21 \pm 0.03$, where the error is due to statistics and the uncertainty on the branching fraction only.

The CLEO fit parameters are also consistent with, and of comparable precision to, those obtained from similar fits by the ALEPH Collaboration [17] to their $\tau^- \to \pi^-\pi^0\nu_\tau$ sample, also shown in Table I. Here also a direct comparison is difficult because the ALEPH fit fixes the width of the $\rho'$ to the PDG value [16] for the $\rho'(1450)$, but allows a $\rho''$ component, with the relative coupling $\gamma$ floating (they obtain $\gamma = -0.015 \pm 0.008$). Fitting the CLEO data to the same function results in only slightly shifted parameters from the results obtained with the nominal fit.

The fits to CLEO and ALEPH $\tau$ data represent the most statistically precise determinations of the charged $\rho$ meson mass and width to date [16]. Furthermore, as alluded to earlier, the analyses of $\tau$ data are free from the complications of strong dynamics in the production, which affect the samples of hadro-produced charged $\rho$ mesons that until now have been the main source of charged $\rho$ data. However, like all other determinations of $\rho$ parameters, interpretation of the results from fits to $\tau$ data are only valid within the context of the specific model used to describe the lineshape.

### B. Systematic Errors

Systematic errors are listed in Table II. We discuss the most significant sources of error below.

#### *1. Bin migration correction*

The resolution on $M_{\pi^-\pi^0}$ (10–20 MeV over the relevant mass range) is dominated by the photon energy measurement. The excellent agreement between data and MC seen in the $\pi^0$

TABLE II. Systematic errors, in MeV except for $\beta$.

| Source | $M_\rho$ | $\Gamma_\rho$ | $\beta$ | $M_{\rho'}$ | $\Gamma_{\rho'}$ |
|---|---|---|---|---|---|
| Backgrounds | 0.1 | 0.5 | 0.002 | 1 | 5 |
| Bin Mig. | 0.3 | 0.5 | 0.001 | 5 | 16 |
| Efficiency | 0.1 | 0.1 | 0.003 | 1 | 5 |
| Fit Proc. | 0.1 | 0.2 | $< 0.001$ | 1 | 1 |
| Mom. Scale | 0.3 | 0.1 | $< 0.001$ | 1 | 1 |
| Energy Scale | 0.8 | 0.2 | $< 0.001$ | 2 | 1 |
| Total Syst. | 0.9 | 0.8 | 0.004 | 6 | 18 |
| Stat. Error | 0.7 | 1.4 | 0.008 | 10 | 39 |

mass spectra in Figure 1 gives us confidence that this resolution function is adequately simulated. That the MC correctly models radiative effects is tested by comparing characteristics of photon-like showers accompanying the $\pi^-\pi^0$ system with those in the data.

The method applied to unfold these effects relies on the approximate similarity between the $M_{\pi^-\pi^0}$ lineshape used as input to the MC and the true one. We have estimated the bias resulting from the inaccuracy of this approximation, and find it to be small. Considering this bias and possible errors in the modeling of the effects themselves, we conservatively arrive at the uncertainties shown in Table II. For reference, failure to correct for bin migration results in values for $M_\rho$ and $\Gamma_\rho$ which are 2.6 MeV lower and 4.6 MeV higher, respectively. Thus we claim to know this correction to $\sim 10\%$ of itself.

### *2. Energy and momentum scales*

Although the $\pi^0$ mass resolution function is well modeled, even a small error in the absolute energy calibration of the calorimeter can have a large effect on $M_\rho$, without disturbing the agreement in Figure 1. Based on studies of photons from various processes, we believe this calibration to be good to better than 0.3%. Scaling the photon energies in the data by a factor of $1 \pm 0.003$ and fitting the $M_{\pi^-\pi^0}$ spectra thus obtained results in the uncertainties shown in Table II. The same procedure is used to assess the systematic error due to the absolute momentum scale uncertainty.

### *3. Background subtraction*

We rescale the individual background components by amounts consistent with uncertainties in branching fractions and detection efficiency. Typically, this is $\pm 10\%$ of the nominal. The largest change in fit parameters comes about by varying the $\tau^- \to K^-\pi^0\nu_\tau$ contribution by this amount. This dominates the error assigned to uncertainties in background subtraction.

*4. Other sources of error*

Other sources of error considered include possible systematic effects in the fit procedure, and in the modeling of the mass-dependence of the acceptance. These uncertainties have been estimated, and they are also shown in Table II.

### C. Model Dependence

As noted earlier, the $\rho$ and $\rho'$ resonance parameters rely on the model used to extract them from the data. We do not include such model dependence in the estimate of systematic errors described above, but we have looked at several specific modifications of our fit function.

First, we consider the inclusion of a $\rho''(1700)$ contribution, which is seen to be important for fits to the $e^+e^- \to \pi^+\pi^-$ data [3,18]. We take input values from the PDG [16] for the $\rho''$ mass and width, and let the admixture fraction ($\gamma$ in Eq. 4) float in the fit. The results for this fit are compared with those from the nominal fit in Table III. We find $\gamma = 0.010 \pm 0.007$, which lies between the values obtained by K&S ($-0.037$) [3] and the DM2 collaboration ($0.053 \pm 0.003$) [18]. The inclusion of $\rho''$ does not strongly affect the fits to the $\tau$ data, which is not surprising given the limited phase space at high mass where the lineshape is most affected.

TABLE III. Results for $\tau^- \to \pi^-\pi^0\nu_\tau$ fits to various models. The first column gives the results for the fit to the nominal model; the second and third correspond to fits with a $\rho''(1700)$ contribution, and with a Blatt-Weisskopf barrier factor in the $q^2$ dependence of the widths, respectively. All values are in units of MeV except for $\beta$ . The errors shown are those due to statistics only.

| | Nominal | w/$\rho''(1700)$ | w/Barrier |
|---|---|---|---|
| $M_\rho$ | $774.3 \pm 0.7$ | $774.2 \pm 0.7$ | $767.7 \pm 0.8$ |
| $\Gamma_\rho$ | $149.1 \pm 1.4$ | $149.2 \pm 1.4$ | $144.1 \pm 1.5$ |
| $M_{\rho'}$ | $1370 \pm 10$ | $1364 \pm 8$ | $1312 \pm 10$ |
| $\Gamma_{\rho'}$ | $386 \pm 39$ | $369 \pm 25$ | $425 \pm 27$ |
| $\beta$ | $-0.091 \pm 0.008$ | $-0.104 \pm 0.007$ | $-0.173 \pm 0.013$ |
| $\chi^2$/dof | 22.4/34 | 21.8/33 | 21.1/32 |

Second, we consider inclusion of a barrier factor $(1 + R^2p_0^2)/(1 + R^2p^2)$ in the expression for the energy dependence of the $\rho$ and $\rho'$ widths $\Gamma_\rho(q^2)$ and $\Gamma_{\rho'}(q^2)$. Here $p$ represents the $\pi$ momentum in the $\pi\pi^0$ rest frame, $p_0$ is the momentum at $q^2 = M_\rho^2$, and $R$ is the *range* parameter, which is roughly expected to be the size of the meson. Some difference of opinion exists as to whether such a factor is well-motivated for describing meson widths (*e.g.*, see Refs. [19,20]). Nonetheless, the determinations of $\rho$ meson parameters which dominate the PDG averages include the barrier factor in their parametrization of the lineshape (see *e.g.*, Ref. [21]). The results from the fit to this model are given in the last column of Table III. We also let the range parameters float in the fit and obtain $R_\rho = 2.5 \pm 0.2$ GeV$^{-1}$ and $R_{\rho'} = 6.3 \pm 3.5$ GeV$^{-1}$.

### D. Comparison with $e^+e^- \to \pi^+\pi^-$ Data

The results from our fit agree with those from similar fits to $e^+e^-$ data, as shown in Table I. Independent of any model, direct comparison between $\tau$ and $e^+e^-$ data can be made as a further test of CVC. To do this we use Eqs. 1 and 2 to represent the fully corrected $\pi^-\pi^0$ mass spectrum in terms of $|F_\pi|^2$, which is plotted with $e^+e^-$ data in Figure 4. A small ($< 1\%$)

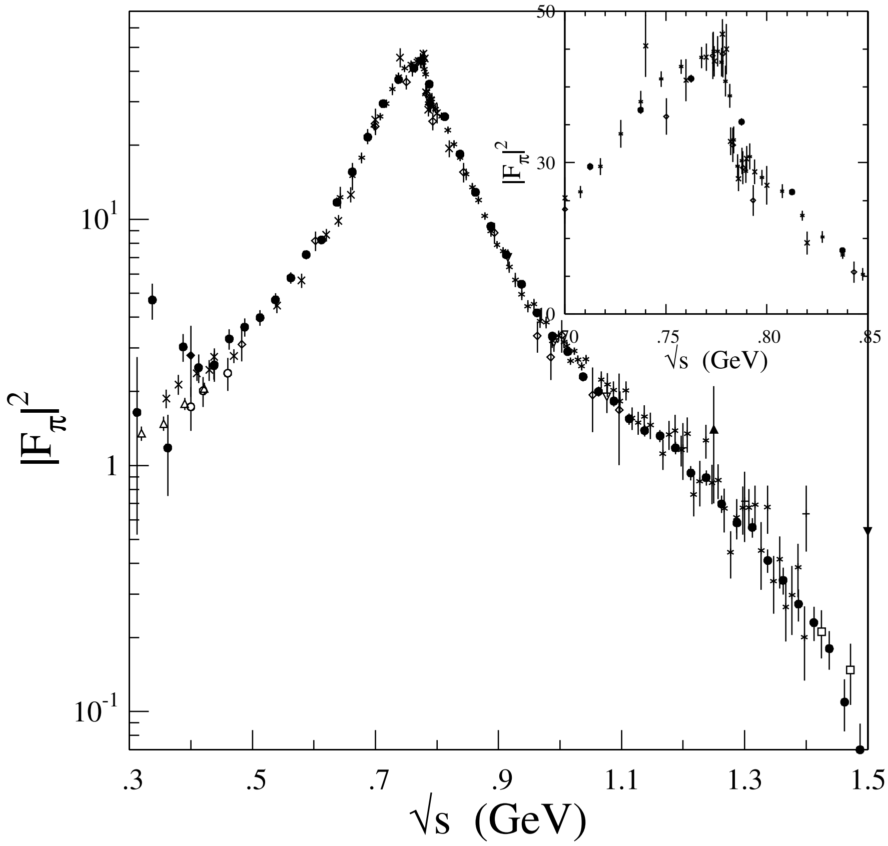


FIG. 4. Comparison of $|F_\pi|^2$ as determined from CLEO-II $\tau^- \to \pi^-\pi^0\nu_\tau$ data (filled circles), with that obtained from $e^+e^- \to \pi^+\pi^-$ cross-sections (other symbols) from OLYA, CMD, M2N, DM1, DM2, NA7, and Adone experiments. The inset is a blow-up of the region near the $\rho$ peak, where $\rho$-$\omega$ interference is evident in the $e^+e^-$ data.

correction is made to the $\tau$ data in this plot to represent it as an unbinned spectrum, using the fit function described earlier to estimate the effect of the lineshape variation across each of the histogram bins. The model-dependence in this correction is completely negligible. The $\tau$ data follow the $e^+e^-$ data shape well, except in the region where $\rho$-$\omega$ interference affects the $e^+e^-$ data. Also, the $\rho$ peak appears broader in the $\tau$ data, as reflected by the larger fit value for $\Gamma_\rho$.

## V. THE $K_S\pi^-$ MASS SPECTRUM

We perform a similar analysis of the $K_S\pi^-$ mass spectrum in $\tau^- \to K_S\pi^-\nu_\tau$ decays. In this case, because of the narrowness of the $K^*(892)$ meson and the considerably smaller statistics than in the $\pi^-\pi^0$ case, we use non-uniform bin-widths for the mass histogram.

We apply the same corrections as in the $\pi^-\pi^0$ case: subtract backgrounds, correct for bin migration, and correct for the mass-dependence of the acceptance. The $K_S\pi^-$ mass spectrum is plotted, before application of these corrections, in Figure 5, with the corresponding MC plot overlaid. The data shape agrees well with the MC expectation, however the MC spectrum peaks at a lower value of $M_{K_S\pi}$ than what is observed in the data.

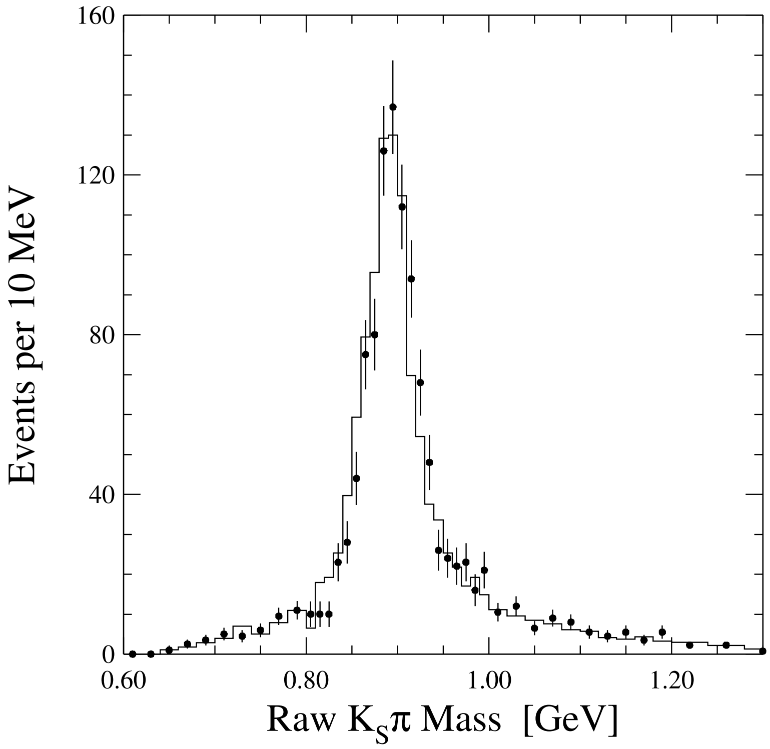


FIG. 5. Reconstructed $K_S\pi^-$ invariant mass spectrum (points), prior to application of corrections described in the text. The corresponding Monte Carlo distribution is overlaid (solid histogram).

The fit to the fully corrected mass spectrum is illustrated in Figure 6. Because of limited statistics, there is not much sensitivity to $K^{*\prime}$ contributions. Thus we fix the mass and width to the PDG values for the $K^*(1410)$, but allow the admixture fraction $\beta_{K^{*\prime}}$ to float in the fit.

The fit results are shown in Table IV. The $K^*$ parameters determined from $\tau$ data are not competitive with those from other sources. At present, we do not understand the shift in $M_{K^*}$. Finally, we do not see evidence of a contribution from the $K^*(1410)$ with the present level of sensitivity.

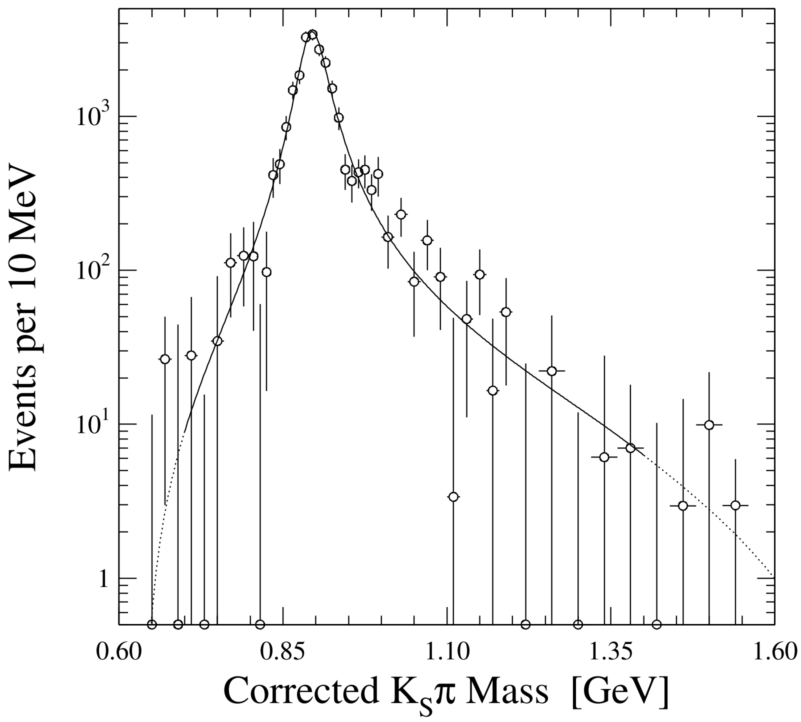


FIG. 6. Fully corrected $M_{K_S\pi^-}$ spectrum (points), with fit function overlaid.

TABLE IV. Fit results for $\tau^- \to K_S\pi^-\nu_\tau$, in MeV except for $\beta_{K^{*\prime}}$. Only statistical errors are shown. Also given are the corresponding PDG values.

| | CLEO-II | PDG |
|---|---|---|
| $M_{K^*}$ | $896.7 \pm 1.4$ | $891.6 \pm 0.2$ |
| $\Gamma_{K^*}$ | $46.4 \pm 3.1$ | $49.8 \pm 0.8$ |
| $\beta_{K^{*\prime}}$ | $-0.02 \pm 0.05$ | — |
| $\chi^2/\mathrm{dof}$ | $39.1/36$ | — |

## VI. CONCLUSIONS

To summarize, we have used data obtained with the CLEO-II detector to study the hadronic mass spectrum in the decays $\tau^- \to \pi^-\pi^0\nu_\tau$ and $\tau^- \to K_S\pi^-\nu_\tau$. Within the context of a simple model we derive the resonance parameters of the lowest lying charged vector mesons $\rho^-(770)$ and $K^{*-}(892)$, and explore possible contributions from radial excitations $\rho'(1450)$ and $K^{*\prime}(1410)$.

Comparison of fit results, as well as of the spectra themselves, between the CLEO $\tau^- \to \pi^-\pi^0\nu_\tau$ data and data from other experiments on $e^+e^- \to \pi^+\pi^-$ supports CVC. The $\tau$ data from CLEO and ALEPH [17] now provide the most precise information on the charged $\rho$ meson lineshape. We also observe structure in the $\pi^-\pi^0$ mass spectrum consistent with interference between $\rho$ and $\rho'$ mesons, at a similar level to that observed in the $e^+e^-$ data.

With a smaller sample of $\tau^- \to K_S\pi^-\nu_\tau$ events, we have studied the $M_{K_S\pi^-}$ spectrum. Unlike in the $\pi^-\pi^0$ case, no evidence is found for production of radial excitation states such as the $K^*(1410)$, however the sensitivity is limited by lack of statistics.

## ACKNOWLEDGEMENTS

We gratefully acknowledge the effort of the CESR staff in providing us with excellent luminosity and running conditions. J.P.A., J.R.P., and I.P.J.S. thank the NYI program of the NSF, M.S. thanks the PFF program of the NSF, G.E. thanks the Heisenberg Foundation, K.K.G., M.S., H.N.N., T.S., and H.Y. thank the OJI program of DOE, J.R.P., K.H., M.S. and V.S. thank the A.P. Sloan Foundation, R.W. thanks the Alexander von Humboldt Stiftung, and M.S. thanks Research Corporation for support. This work was supported by the National Science Foundation, the U.S. Department of Energy, and the Natural Sciences and Engineering Research Council of Canada.

## REFERENCES


[1] Application to charge-conjugate reactions is implied throughout this paper.
[2] Y.S. Tsai, Phys. Rev. D **4**, 2821 (1971).
[3] J.H. Kühn and A. Santamaria, Z. Phys. C **48**, 445 (1990).
[4] M. Finkemeier, in *Proceedings of the Fourth Workshop on Tau Lepton Physics*, Estes Park, Colorado, 1996, edited by J. G. Smith and W. Toki [Nucl. Phys. B (Proc. Suppl.) **55C**, 325 (1997)].
[5] E. Mirkes, in *Proceedings of the Fourth Workshop on Tau Lepton Physics*, Estes Park, Colorado, 1996, edited by J. G. Smith and W. Toki [Nucl. Phys. B (Proc. Suppl.) **55C**, 169 (1997)].
[6] M. Finkemeier and E. Mirkes, Z. Phys. C **69**, 243 (1996).
[7] $h^-$ is used to denote $\pi^-$ or $K^-$.
[8] Y. Kubota *et al.* (CLEO Collaboration), Nucl. Instrum. Methods A **320**, 66 (1992).
[9] M. Artuso *et al.* (CLEO Collaboration), Phys. Rev. Lett. **72**, 3762 (1994).
[10] T.E. Coan *et al.* (CLEO Collaboration), Phys. Rev. D **53**, 6037 (1996).
[11] `KORALB 2.1 / TAUOLA 1.5`: S. Jadach and Z. Was, Comput. Phys. Commun. **36**, 191 (1985), **64**, 267 (1991); S. Jadach, J.H. Kühn, and Z. Was, Comput. Phys. Commun. **64**, 275 (1991), **70**, 69 (1992), **76**, 361 (1993).
[12] `GEANT 3.15`: R. Brun *et al.*, CERN DD/EE/84-1.
[13] `PHOTOS 2.0`: E. Barberio and Z. Was, Comput. Phys. Commun. **79**, 291 (1994).
[14] L.M. Barkov *et al.*, Nucl. Phys. B **256**, 365 (1985).
[15] S. Eidelman, in *Proceedings of the Fourth Workshop on Tau Lepton Physics*, Estes Park, Colorado, 1996, edited by J. G. Smith and W. Toki [Nucl. Phys. B (Proc. Suppl.) **55C**, 181 (1997)].
[16] R.M. Barnett *et al.*, (Particle Data Group), Phys. Rev. D **54**, 1 (1996).
[17] R. Barate *et al.* (ALEPH Collaboration), CERN-PPE/97-013, 1997.
[18] D. Bisello *et al.* (DM2 Collaboration), Phys. Lett. B **220**, 321 (1989).
[19] A.B. Clegg and A. Donnachie, Z. Phys. C **62**, 455 (1994).
[20] M. Benayoun *et al.*, Z. Phys. C **58**, 31 (1993).
[21] J. Pisut and M. Roos, Nucl. Phys. B **6**, 325 (1968).